Cell

Reversal of Cancer Cachexia and Muscle Wasting by ActRIIB Antagonism Leads to Prolonged Survival

Xiaolan Zhou,[1] Jin Lin Wang,[1] John Lu,[1] Yanping Song,[1] Keith S. Kwak,[1] Qingsheng Jiao,[1] Robert Rosenfeld,[1] Qing Chen,[1] Thomas Boone,[1] W. Scott Simonet,[1] David L. Lacey,[1] Alfred L. Goldberg,[2] and H.Q. Han[1,*]

[1]Departments of Metabolic Disorders and Protein Science, Amgen Research, Thousand Oaks, CA 91320, USA
[2]Department of Cell Biology, Harvard Medical School, Boston, MA 02115, USA
*Correspondence: hqhan@amgen.com
DOI 10.1016/j.cell.2010.07.011

SUMMARY

Muscle wasting and cachexia have long been postulated to be key determinants of cancer-related death, but there has been no direct experimental evidence to substantiate this hypothesis. Here, we show that in several cancer cachexia models, pharmacological blockade of ActRIIB pathway not only prevents further muscle wasting but also completely reverses prior loss of skeletal muscle and cancer-induced cardiac atrophy. This treatment dramatically prolongs survival, even of animals in which tumor growth is not inhibited and fat loss and production of proinflammatory cytokines are not reduced. ActRIIB pathway blockade abolished the activation of the ubiquitin-proteasome system and the induction of atrophy-specific ubiquitin ligases in muscles and also markedly stimulated muscle stem cell growth. These findings establish a crucial link between activation of the ActRIIB pathway and the development of cancer cachexia. Thus ActRIIB antagonism is a promising new approach for treating cancer cachexia, whose inhibition per se prolongs survival.

INTRODUCTION

Cancer cachexia affects up to 80% of patients with advanced cancers and accounts for nearly 30% of cancer-related deaths (Acharyya et al., 2005; Fearon, 2008; Tisdale, 2009). However, few therapeutic options are currently available for cancer cachexia. A key feature of cachexia is the progressive depletion of skeletal muscle mass, which occurs in concert with the loss of body fat. Muscle wasting dramatically reduces the quality of life but also appears to correlate with fatal outcomes. The mechanism by which cancers provoke the loss of the host's muscle mass is presently thought to be multifactorial. Various hormones, cytokines and tumor-derived factors have been shown to influence muscle protein balance in normal and disease states, through several major intracellular signal transduction systems. While activation of the AKT pathway is associated with muscle

growth, in atrophying muscles there is an activation of FOXO as well as NF-κB and possibly also Smad transcription factors, which promote protein degradation (Glass, 2005; Sandri et al., 2004). FOXO3 by itself induces a set of atrophy-related genes, especially the muscle-specific ubiquitin ligases Atrogin-1 and MuRF1, which promotes breakdown of myofibrillar apparatus, and genes for autophagy (Cohen et al., 2009; Zhao et al., 2007). However, it remains unclear which of these signaling systems plays a dominant role in the pathogenesis of cancer-associated muscle loss.

ActRIIB is a high affinity activin type 2 receptor and mediates the signaling by a subset of TGF-β family ligands including myostatin, activin, GDF11 and others (Lee & McPherron, 2001; Souza et al., 2008). Expression of a dominant negative ActRIIB in transgenic mice results in skeletal muscle hypertrophy, suggesting an important role of ActRIIB pathway in limiting muscle growth (Lee & McPherron, 2001). Myostatin null mutations also lead to skeletal muscle hypertrophy in multiple species including humans, whereas forced myostatin overexpression in adult mice leads to systemic muscle wasting (Schuelke et al., 2004; Zimmers et al., 2002). In addition, in inhibin-deficient mice, activins are deregulated, leading to gonadal tumors and marked cachexia (Matzuk et al., 1994). Therefore, ActRIIB ligands appear critical in regulating muscle mass (Lee et al., 2005).

Increased signaling by the ActRIIB pathway has been implicated in many cancers (Costelli et al., 2008; Harada et al., 1996; Otani et al., 2001; Petraglia et al., 1998; Seder et al., 2009; Thomas, et al., 1997; Wildi et al., 2001), but its possible importance in pathogenesis of cancer cachexia remain obscure. In these investigations we set out (1) to examine in animal models of cancer cachexia the possible therapeutic impact of blocking ActRIIB pathway on muscle wasting and survival, and (2) to define the mechanisms by which ActRIIB pathway may modify the course of cancer cachexia. To antagonize the ActRIIB pathway activity, we have administered an ActRIIB decoy receptor referred to as sActRIIB in multiple cancer cachexia models, including the colon 26 (C26) tumor-bearing mice and inhibin-deficient mice, as well as nude mice bearing human G361 melanoma and TOV-21G ovarian carcinoma xenografts. Bearing tumors of distinctly different origins, these models mimic human cancer cachexia with a promounced

loss of muscle mass at low tumor burden and display a dramatic wasting that is eventually lethal (Matzuk et al., 1994; Mori et al., 1991; Tanaka et al., 1990). The present studies demonstrate that sActRIIB not only prevents further wasting, but also fully reverses skeletal muscle loss and atrophy of the heart, thereby dramatically prolonging survival of the tumor-bearing animals. Importantly, in the C26 model, these marked effects are seen even without any effect on tumor growth, adiposity, or levels of inflammatory cytokines. Our data reveal that ActRIIB antagonism reverses wasting by blocking the activation of muscle protein breakdown and stimulating muscle stem cell growth. Thus, ActRIIB pathway inhibition appears to have therapeutic potential for treating various types of muscle wasting, especially cancer cachexia.
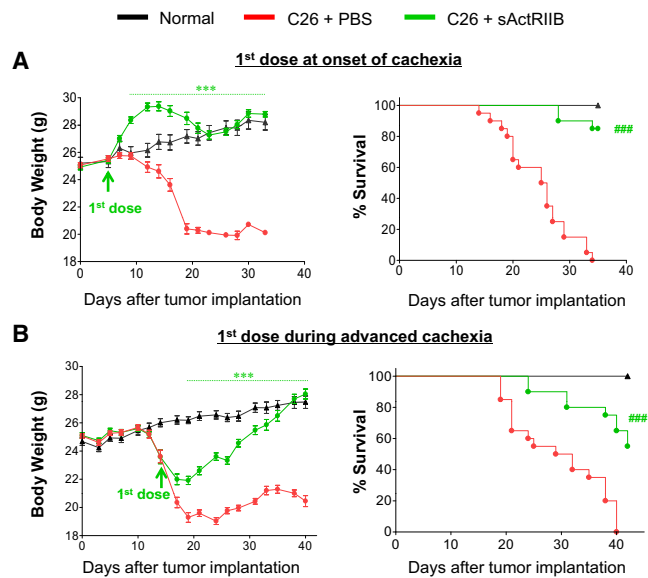
RESULTS

sActRIIB Is a Potent Inhibitor of Myostatin and Activin A Signaling

We measured the ligand-neutralizing activities of recombinant sActRIIB using C2C12 myoblasts stably transfected with a luciferase reporter for Smad2/3 signaling, as detailed in Experimental Procedures. sActRIIB potently inhibited both myostatin- and activin-mediated Smad2/3 signal transduction with IC_{50} values around 1.1 nM against myostatin and 3.6 nM against activin A (Figure S1A available online). The half-life ($T_{1/2}$) of sActRIIB in mice was longer than 10 days. Administration of of a single dose of sActRIIB to adult C57Bl/6 mice led to dose-dependent increases in body weight and lean body mass (Figure S1B).

ActRIIB Antagonism Reverses Muscle Loss and Prolongs Survival in C26 Tumor-Bearing Mice

The C26 tumor implanted mice manifested a lethal wasting syndrome characterized by progressive weight loss and death (Tanaka et al., 1990). As shown in Figure 1A, weight loss in these tumor-bearing mice began around day 5 after implantation, and within 2–3 weeks of implantation, their body weights declined by > 20%. Analysis of individual body weight changes indicates that when the tumor-free body weight decreased by > 25% after the tumor implantation (i.e., by > 35% compared to the normal control mice), deaths occurred (Figure S2). We administered sActRIIB to this model at different stages of cachexia and analyzed the changes in body weights and survival rates. When administration was begun when weight loss first became evident, weekly injection of sActRIIB not only completely prevented further weight loss, but even caused a rapid gain in body weight which soon exceeded that in non-implanted control mice (Figure 1A). Furthermore, when treatment was initiated during advanced cachexia, when more than 10% body weight was lost, the sActRIIB treatment rapidly and fully reversed the weight loss back to weights of normal control mice (Figure 1B). Remarkably, the gains in body weight were associated with a profound prolongation of survival in the tumor-bearing animals (p < 0.0001) (Figures 1A and 1B). Thus, regardless of the timing of the first dose during the course of cachexia, sActRIIB was able to reverse weight loss completely and to prolong animal survival dramatically.

Figure 1. Changes in Body Weights and Survival Rates in C26 Tumor-Bearing Mice Resulting from sActRIIB Administered at Different Stages of Cachexia

Arrows point to the timings of the 1st dose at day 5 (A) and day 14 (B) post tumor implantation, respectively, in two separate experiments. C26 mice were treated with sActRIIB (10 mg/kg, SC, weekly) or PBS (n = 20). Age-matched normal control mice were treated with PBS (n = 10). ***p < 0.001; ###p < 0.0001.

See also Figures S1 and S2.

sActRIIB Restores Mass and Strength of Atrophying Muscle without Affecting Tumor Growth or Fat Loss in C26-Bearing Mice

Body composition analysis further demonstrated that sActRIIB completely blocked the loss of lean body mass, but surprisingly did not inhibit the decrease in fat mass in the C26 mice (Figure 2A). The weights of extensor digitalis longus (EDL), soleus, calf and tibialis anterior (TA) muscles in the untreated C26 mice decreased by more than 25% below levels in normal controls. However, the weights of all these muscles in sActRIIB-treated C26 mice were similar to or even greater than those in controls. Thus, the treatment fully protected the fast-twitch (EDL), slow-twitch (soleus) and mixed-fiber (calf and TA) muscles against cancer-associated atrophy (Figure 2A). Furthermore, the grip strength of the untreated C26 mice declined in parallel with the muscle weights. However, the sActRIIB treatment completely restored grip strength to above the normal levels (Figure 2B). Thus, the sActRIIB treatment caused a buildup of functional muscle in the tumor-bearing animals to levels resembling or exceeding control levels.

To monitor possible effects of sActRIIB on growth of the C26 tumor, we measured tumor sizes and weights. As shown in Figure 2C, sActRIIB treatment had no effect on C26 tumor growth rate or weight. Thus, the dramatic muscle sparing is clearly not due to elimination of the primary tumor. Also, because neither fat mass nor tumor growth was affected by the treatment, the prolongation of survival in the C26 mice must be attributable to the large muscle sparing effect of sActRIIB. Therefore,
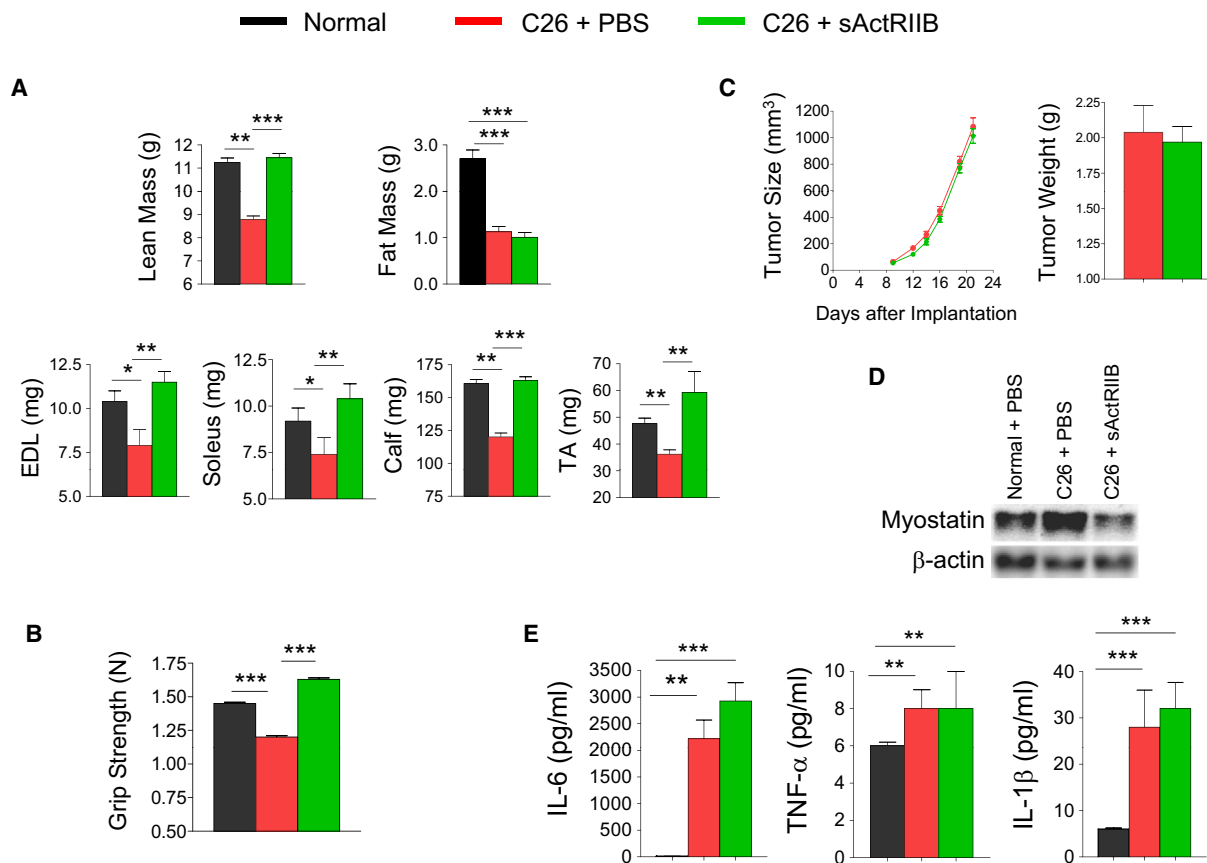
Figure 2. ActRIIB Antagonism Reverses Muscle Wasting in C26 Tumor-Bearing Mice without Affecting Tumor Growth, Fat Loss, or Inflammatory Cytokine Levels

(A) sActRIIB prevents loss of lean muscle mass but has no effect on fat loss in C26 mice. Body composition was analyzed at day 25 post tumor implantation.
(B) sActRIIB restores the grip strength of C26 mice beyond normal control level. Grip strength was measured prior to necropsy.
(C) sActRIIB treatment does not alter C26 tumor growth. Tumor sizes were measured longitudinally and tumor weights were measured by necropsy.
(D) Northern blot analysis on myostatin expression in gastrocnemius muscles.
(E) ELISA on serum levels of IL-6, TNF-α and IL-1β.
Values are means ± SEM. *p < 0.05, **p < 0.01; ***p < 0.001. n = 10-12.
See also Table S1.

sActRIIB was able to extend the survival by reversing cachexia even without inhibiting tumor growth.

sActRIIB Blocks Myostatin Overproduction in C26 Model but Does Not Reduce Elevated Levels of IL-6, IL-1β, or TNF-α

Northern blot analysis of the gastrocnemius muscles of C26-bearing mice revealed that myostatin mRNA level increased by more than 2-fold over control level, but sActRIIB treatment prevented this induction of myostatin (Figure 2D). However, no change in activin A (βA) mRNA level was detected in the gastrocnemius (data not shown). This induction of myostatin in muscle apparently was triggered by humoral mediator(s) either secreted by the C26 tumor, which was implanted subcutaneously, or released by the host in response to the tumor burden. Because sActRIIB treatment fully abolished the myostatin overexpression, activation of ActRIIB pathway must be critical for its induction.

It is widely believed that proinflammatory cytokines are critical in the development of cancer cachexia (Argiles & Lopez-Soriano, 1999). To test whether sActRIIB treatment might be achieving its anti-cachexia effect by attenuating proinflammatory cytokines, we measured by ELISA the serum levels of IL-6, IL-1β and TNF-α in the C26 mice. As reported previously, these major cytokines, especially IL-6, were elevated in the circulation in C26 mice (Strassmann et al., 1992; Tanaka, et al., 1993). Unexpectedly, the sActRIIB treatment did not change the levels of these cytokines (Figure 2E), and thus they cannot account for the reversal of cachexia seen upon sActRIIB treatment. These findings imply that increased levels of IL-6 by itself can not induce the cachectic syndrome. To test this conclusion, we treated normal adult mice with a pharmacological dose of recombinant IL-6 by continuous infusion, but found no significant change in either body weight or muscle mass (Table S1). Thus, in the C26 model, ligands of the ActRIIB pathway appear to be

more important than proinflammatory cytokines in triggering muscle wasting and cachexia.

ActRIIB Antagonism Reverses Muscle Wasting, Ameliorates Anorexia, and Prolongs Survival in Inhibin-Deficient Mice

To examine whether ActRIIB pathway blockade is also effective in reversing muscle wasting induced by other cancers, we administered sActRIIB to inhibin-α knockout (KO) mice, which spontaneously form gonadal tumors and manifest marked cachexia (Matzuk et al., 1994). It has been reported that genetic crossing of inhibin-α KO mice with follistatin transgenic or ActRII (ActRIIA) KO mice slows both tumor formation and development of weight loss (Cipriano et al., 2000; Coerver et al., 1996). Also, administration of ActRIIA-Fc (a soluble receptor different from the sActRIIB studied here) to 3-week-old inhibin-deficient mice (when neither cachexia nor tumor was evident) had similar beneficial effects on body weight and tumor growth (Li et al., 2007). Thus, blocking deregulated activins before disease onset in inhibin-deficient mice slowed the development of tumor cachexia. However, it is unclear whether inhibiting activins after tumors and weight loss have fully developed in these mice could have any beneficial effect on tumor growth, cachexia, or both. This question is of therapeutic importance, since cachexia is generally found in patients with advanced cancers. Also, none of these studies examined muscle wasting, the most debilitating aspect of cachexia. Here, we administered sActRIIB to the inhibin-α KO mice after tumor cachexia had advanced to a late stage and analyzed the effects on muscle wasting, anorexia and survival.

By 8 weeks of age, the weights of the male and female inhibin-α KO mice were 10%–17% lower than those of age-matched wild-type (WT) controls. We initially administered sActRIIB to the KO mice at 8 weeks of age. The WT mice grew steadily while the untreated KO mice of both sexes suffered dramatic weight loss, and nearly all died within a 10-week period (Figure 3A). It should be noted that the plot of the weights of the surviving KO mice against time (Figure 3A) underestimates the actual weight loss of the inidividual untreated KO mice, because those animals showing greatest weight loss died sooner and thus steadily dropped out from the plots of mean body weights. In fact, individual body weight analysis indicates that at death, the untreated KO mice had lost an average of 24% (p < 0.001) of their initial body weights (i.e., at 8 weeks of age), and their mean muscle mass diminished to less than 50% of that of WT control (p < 0.001) (Figure S3A). However, within one week of treatment with sActRIIB, the body weights of both male and female KO mice increased rapidly and reached levels in the WT littermates. With continued sActRIIB treatment, their body weights even exceeded the WT controls (Figure 3A). Remarkably, along with the body weight improvement, a dramatic prolongation in survival was observed in the sActRIIB-treated KO mice (p < 0.0001). In fact, when 100% of the untreated male and female KO mice had died, nearly all the treated males and 85% of the treated females were still alive (Figure 3A).

To test the ability of sActRIIB to reverse muscle loss and cachexia-anorexia syndrome, we then administered a single dose to 8-week-old male and 12-week-old female KO mice. By these ages, gonadal tumors and cachexia had developed to an advanced stage in these KO mice with the animals loosing about 22%–28% of their muscle mass compared to their WT controls (Figure S3B). We analyzed the mice 14 days after the single dose. In the absence of sActRIIB treatment, body weights, food intake, lean body mass, fat mass, and mass of the gastrocnemius in the male and female KO mice were 20%–45% lower than those in the WT controls (Figure 3B and Figure S3C). However, sActRIIB treatment rapidly reversed all these parameters back to or even beyond the levels in the WT controls. Notably, a single injection of sActRIIB was able to cause the doubling of the mass of gastrocnemius muscle in the KO mice within two weeks (Figure 3B).

To determine how these ActRIIB pathway perturbations affect muscle function, we analyzed the myosin heavy chain contents as well as muscle grip strength in the inhibin-α KO mice. As shown by western blot analysis, the content of myosin heavy chain in the gastrocnemius was lower in the untreated KO mice than in WT controls, but after sActRIIB treatment, it was increased to an even higher level than in the WT (Figure 3C). Concomitantly, sActRIIB treatment fully restored the weakened grip strength to above normal control levels (Figure 3D). Thus, sActRIIB promoted a buildup of functional muscle and was highly effective in ameliorating all aspects of the cachexia syndrome, including anorexia and fat loss, in the inhibin-deficient animals.
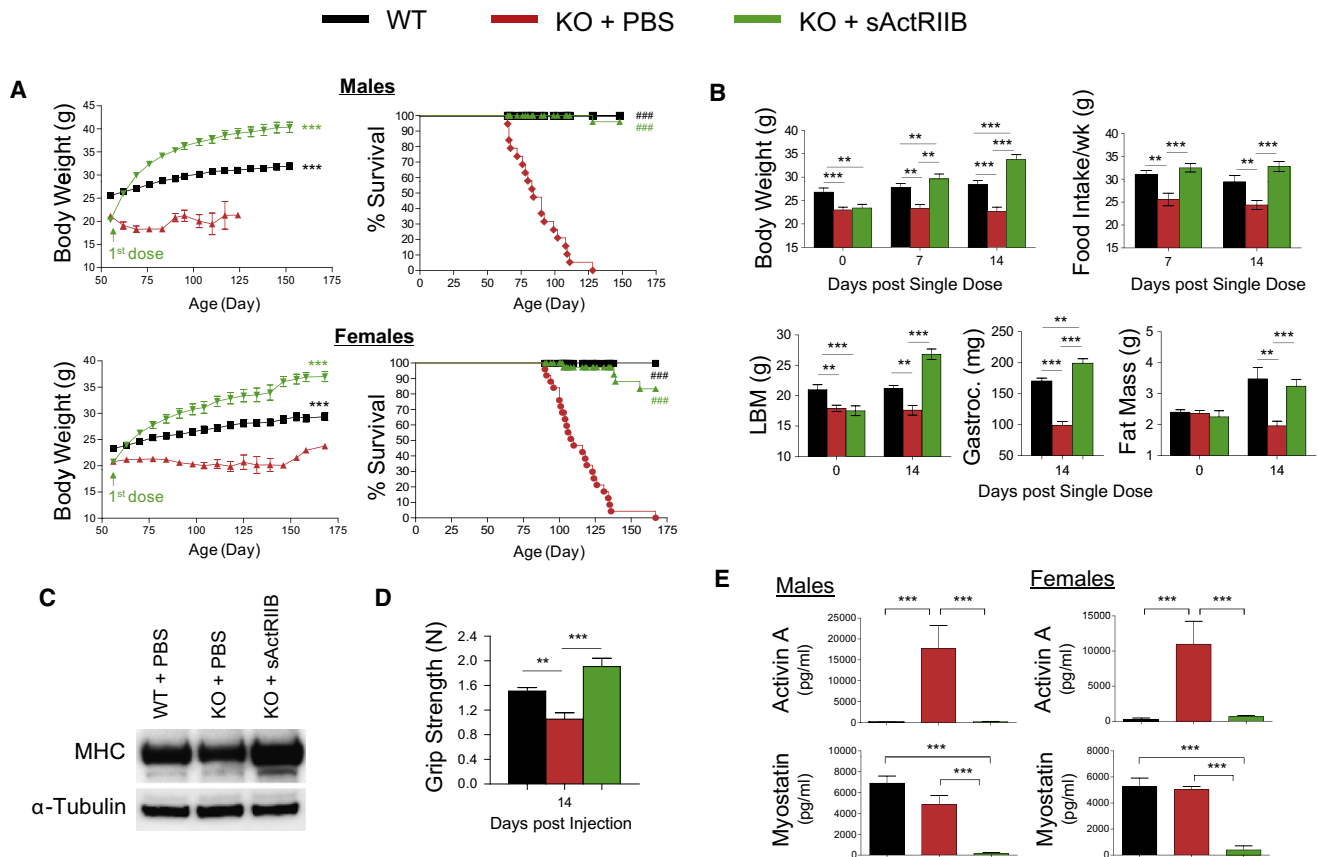
Because of these profound effects on the survival of inhibin-α KO mice, we examined the impact of sActRIIB on the progression of the gonadal tumors, after they had been already established in these male and female KO mice. Surprisingly, a single dose of sActRIIB caused a dramatic suppression of the advanced ovarian and testicular tumors in these mice (Figure S3D).

sActRIIB Sequesters Activin A and Myostatin In Vivo

To understand how ActRIIB ligand levels may change in response to sActRIIB treatment, we measured the amounts of circulating activin A and myostatin in the inhibin-α KO mice. Serum activin A levels were much higher in both male and female KO mice than in WT controls; but, a single dose of sActRIIB completely abolished the increase in activin A within two weeks. By contract, serum myostatin levels in KO mice did not differ significantly from WT levels, but were markedly suppressed by sActRIIB treatment (Figure 3E). Thus, sActRIIB neutralized both activin A and myostatin in vivo, and these actions can account for the therapeutic effects on cachexia, tumorigenesis and survival in the inhibin-deficient animals.

ActRIIB Antagonism Reverses Cancer-Induced Atrophy of the Heart

During cancer cachexia in both the C26 tumor-bearing mice and inhibin-deficient mice with advanced gonadal cancers, there was a marked diminution in heart mass that was evident on necropsy. The average heart weights in these cachectic animals decreased by 20%–29% compared to the normal controls, and a dramatic reduction in ventricular wall thickness was evident upon histological examination of the cardiac cross-sections. Remarkably, sActRIIB treatment completely blocked the cardiac atrophy in both C26 mice and inhibin-deficient mice (Figure 4).

Figure 3. sActRIIB Treatment Completely Reverses Muscle Loss and Anorexia and Dramatically Prolongs Lifespan in Inhibin-α KO Mice

(A) Changes in body weights and survival rates in male and female inhibin-α KO mice in response to sActRIIB. 8-week-old KO mice received either PBS or sActRIIB (10 mg/kg, SC, weekly). Age-matched WT mice received PBS.

(B) Effect of a single dose of sActRIIB on body weight, food intake, body composition and muscle mass in male inhibin-α KO mice. 8-week-old KO mice received a single injection of sActRIIB (30 mg/kg, SC) or PBS. Age-matched WT mice were used as control. Necropsy was performed at 14 days after injection.

(C) Western blot analysis on myosin heavy chain (MHC) contents of gastrocnemius muscles.

(D) A single dose of sActRIIB fully restores the grip strength. Grip strength was measured at day 14.

(E) Changes in serum activin A and myostatin levels in male and female KO mice in response to sActRIIB.

Values are means ± SEM. Survival studies: ###p < 0.0001; n = 20-25 per KO group; n = 17-19 per WT group. Other studies: *p < 0.05, **p < 0.01, ***p < 0.001; n = 10-12.

See also Figure S3.

Thus cardiac atrophy is an important but unappreciated feature of cancer cachexia and seems to result from enhanced ActRIIB signaling. Interestingly, in contrast to our findings in skeletal muscle described below, we found no change in the atrophic hearts in expression of atrophy-specific ubiquitin ligases or in BrdU labeling following sActRIIB treatment (data not shown). Therefore, the biochemical mechanisms of this dramatic cardiac atrophy and re-growth clearly require further investigations.

Elevated Activin Is Critical in the Pathogenesis of Muscle Wasting and Anorexia Associated with Multiple Cancers

To investigate whether elevated activin A can cause cachexia, we implanted adult nude mice with CHO cells that had been transfected with activin A (CHO-Activin). The resulting overproduction of activin A in these xenograft-bearing mice led to progressive weight loss, depressed food intake, muscle wasting, and death (Figure 5A). To verify that this lethal wasting syndrome resulted from the elevated activin A, we administered an anti-activin A antibody to the CHO-Activin implanted mice. This treatment prevented the weight loss, anorexia, muscle wasting and the rapid death of these xenograft-bearing animals (Figure 5A). The CHO-Activin-bearing mice also lost up to 30% of their fat mass (p < 0.01), and this loss was completely prevented by anti-activin A antibody treatment. Thus, elevated activin A can play a causal role in the development of muscle wasting and cachexia-anorexia syndrome.

It is noteworthy that activin overexpression also caused the decrease in food intake in the CHO-Activin implanted mice, since the activin A-neutralizing antibody completely blocked this effect. This finding is consistent with our observation that the depressed food intake in the inhibin-α KO mice was completely
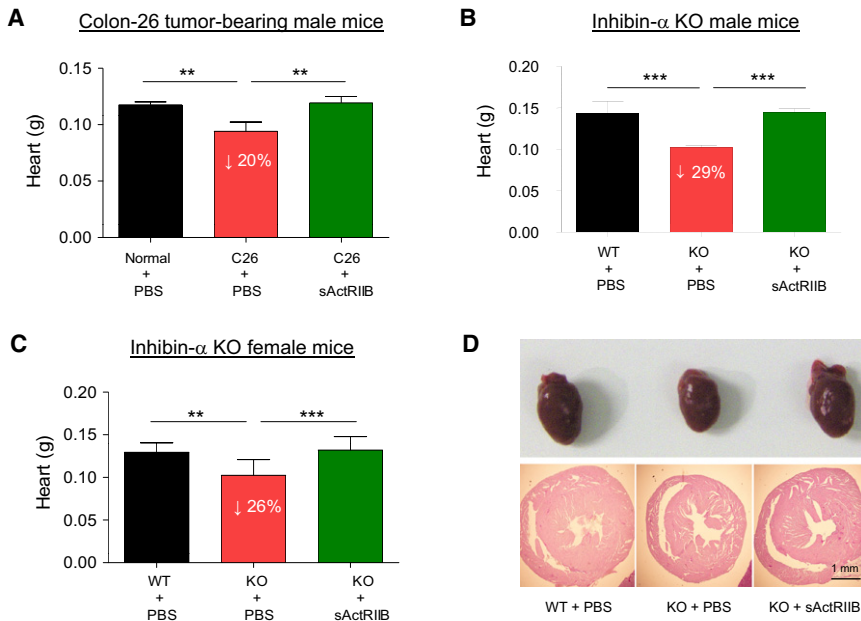
Figure 4. C26 Tumor-Bearing Mice and Inhibin-α KO Mice Show Marked Cardiac Atrophy that Is Completely Reversed by ActRIIB Antagonism

(A) sActRIIB reverses heart atrophy in C26 mice. Cachectic C26 mice were treated with sActRIIB (10 mg/kg, SC, weekly) or PBS. As control, age-matched normal mice received PBS. Heart weights were determined via necropsy after 2 weeks of treatment. Values are means ± SEM. **p < 0.01; n = 6.

(B and C) sActRIIB treatment ameliorates heart atrophy in inhibin-α KO mice. 8-week-old KO males (B) and 12-week-old KO females (C) (both carrying advanced gonadal tumors) were treated with a single dose of sActRIIB (30 mg/kg, SC) or PBS. Age-matched WT males and females were used as normal controls. Heart weights were determined by necropsy 2 weeks after treatment. Values are means ± SEM. **p < 0.01, ***p < 0.001; n = 9-10.

(D) sActRIIB treatment reverses the reduction in ventricular wall thickness in inhibin-α KO mice. Representative images of PAS-stained heart cross-sections from WT (left), untreated KO (middle) and sActRIIB-treated KO (right) mice are shown.

reversed by sActRIIB treatment (Figure 3B). Thus, elevated activin A mediates anorexia, although the mechanism by which activin A regulates food intake is unclear and warrants further investigation.

To determine the importance of this anorexia in mediating activin-induced wasting, we pair fed the CHO-Vector implanted mice with a reduced amount chow equal to that consumed by the CHO-Activin implanted mice. The pair feeding resulted in a loss of about 5% body weight and lean mass in the CHO-Vector implanted mice. By contrast, the CHO-Activin implanted mice lost over 20% of their mean body weight and lean mass during the same period. The pair feeding also had no effect on the survival of the CHO-Vector bearing mice. In contrast, 100% of the CHO-Activin bearing mice died by the end of the experiment (Figure S4A). Thus, although elevated activin A markedly reduces food intake, the decrease in nutrient intake can account for only a minor portion of the body wasting induced by the activin-secreting tumor, and the major fraction of weight loss must be due to activin A-induced tissue catabolism.

To further investigate the role of activin A in the pathogenesis of cancer cachexia, we implanted nude mice with the human ovarian cancer TOV-21G (Provencher et al., 2000) or human melanoma G361 (Mori et al., 1991). These tumor lines were found to secrete in vitro higher amounts of activin A as compared to a variety of other cancer lines examined (Figure 5B). Implantation of these tumors as xenografts in nude mice resulted in significant weight loss, muscle wasting, reduced food intake and fat loss, all of which were fully prevented by sActRIIB treatment (Figures 5C and 5D). In addition, sActRIIB also suppressed the growth of TOV-21G and G361 xenografts in nude mice (Figure S4B). These observations on the activin A-secreting xenograft are similar to our findings on the inhibin-α KO mice and provide further evidence that ActRIIB ligands, especially activin A, are critical in the muscle wasting associated with various cancers as well as in the progression of certain tumors.

ActRIIB Pathway Inhibition Attenuates the Accelerated Muscle Protein Catabolism during Cancer Cachexia

There is mounting evidence that the ubiquitin-proteasome system mediates the breakdown of the bulk of muscle proteins, and its activation accounts for much of the accelerated muscle proteolysis in various catabolic disease states (Cohen et al., 2009; Mitch & Goldberg, 1996). In the atrophying muscles, multiple components of this pathway are induced, including the muscle-specific E3 ligases, Atrogin-1 and MuRF1, and their induction is essential in rapid atrophy (Bodine et al., 2001; Gomes et al., 2001). To determine whether the ActRIIB pathway might regulate these critical components during cancer cachexia, we examined by Northern the levels of ubiquitin (Ub), Atrogin-1 and MuRF1 in gastrocnemius muscles of C26 mice and inhibin-α KO mice (Figure 6A). mRNA levels for these atrophy-related genes in the gastrocnemius were markedly increased above control levels in both cachexia models, but sActRIIB treatment completely abolished their induction (Figure 6A). Thus, antagonism of the ActRIIB pathway prevents the activation of key components of the ubiquitin-proteasome pathway during cancer cachexia.

In various types of muscle atrophy, there is a general acceleration of protein ubiquitination, which is demonstrable in muscle extracts (Kwak et al., 2004; Solomon et al., 1998). To investigate the effects of sActRIIB treatment on muscle protein ubiquitination, we examined rates of ubiquitin conjugation to endogenous proteins in the gastrocnemius from inhibin-α KO mice. As shown in Figure 6B, there was a sharp rise in ubiquitin conjugation in muscle extracts of the KO mice, which was prevented by sActRIIB treatment. Thus, sActRIIB blocked the enhanced
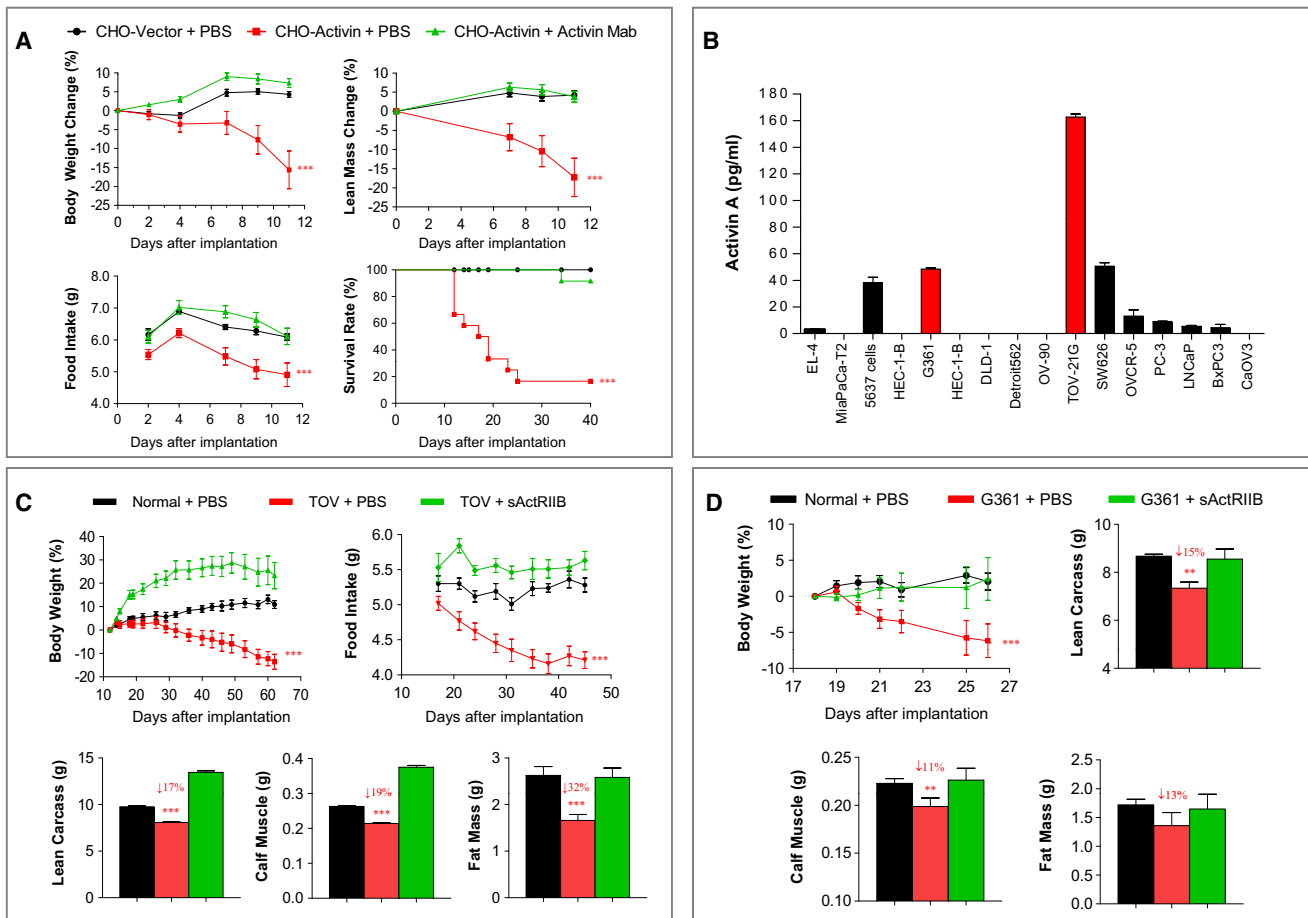
Figure 5. sActRIIB Treatment Prevents the Development of Cachexia-Anorexia Syndrome in Nude Mice Bearing Activin A-Secreting Xenografts

(A) Activin A-overexpressing CHO xenografts results in a lethal muscle wasting-anorexia syndrome in nude mice. Nude mice were each implanted with 3×10^6 CHO-Activin or CHO-Vector cells. CHO-Activin xenograft-bearing mice were treated with activin A antibody (Activin Mab) (20 mg/kg, SC, 2X/week) or PBS. Changes in body weight, lean body mass, food intake and survival rate are shown.

(B) Activin A secretion levels of various human cancer cell lines in vitro. All the cancer cell lines were cultured for 68 hr and the medium was analyzed by ELISA. TOV-21G and melanoma G361 (red) were selected for xenograft studies in nude mice.

(C) sActRIIB prevents weight loss, anorexia, and loss of muscle and adipose tissues in nude mice bearing TOV-21G xenografts.

(D) sActRIIB prevents weight loss, muscle wasting and fat loss in nude mice bearing G361 xenografts.

Values are means ± SEM. **p < 0.01, ***p < 0.001; ***p < 0.0001 on survival rate. n = 12.

See also Figure S4.

ubiquitination in muscle that is characteristic of the cachectic state. To explore the mechanism by which ActRIIB pathway regulates the atrophy-specific ubiquitin ligases, we assayed by western blot the activities of Smad and FOXO signaling systems in muscles of inhibin-α KO and control mice. As expected, phospho-Smad2 was markedly increased in the gastrocnemius of KO mice above levels in WT, and sActRIIB treatment completely blocked this Smad2 activation (Figure 6C).

Smad and FOXO signal transduction systems can influence each other's activity (Seoane et al., 2004), and in skeletal muscle, the myostatin-Smad pathway stimulates FOXO function (Sartori et al., 2009; Trendelenburg et al., 2009). FOXO3 activation has been shown to induce Atrogin-1 and MuRF1 transcription, stimulate proteolysis and cause atrophy (Mammucari et al., 2007;

Sandri et al., 2004; Zhao et al., 2007). Since Smad2 signaling was activated in muscles of the inhibin-α KO mice and suppressed by sActRIIB treatment, we investigated FOXO3 activity in these tissues. Western blot analysis revealed an increase in total FOXO3a content, along with a decrease in the inactive species phospho-FOXO3a in the gastrocnemius of the KO mice, compared to levels in control mice (Figure 6D). These findings indicate FOXO3a activation, since only dephosphorylated FOXO3a enters the nucleus and stimulates transcription. sActRIIB treatment decreased the total FOXO3a content and increased phospho-FOXO3a in the gastrocnemius of the KO mice. This reduction in FOXO activity suggests activation of the PI3K-AKT pathway, which causes FOXO phosphorylation (Figure 6D). Accordingly, western blot analysis demonstrated
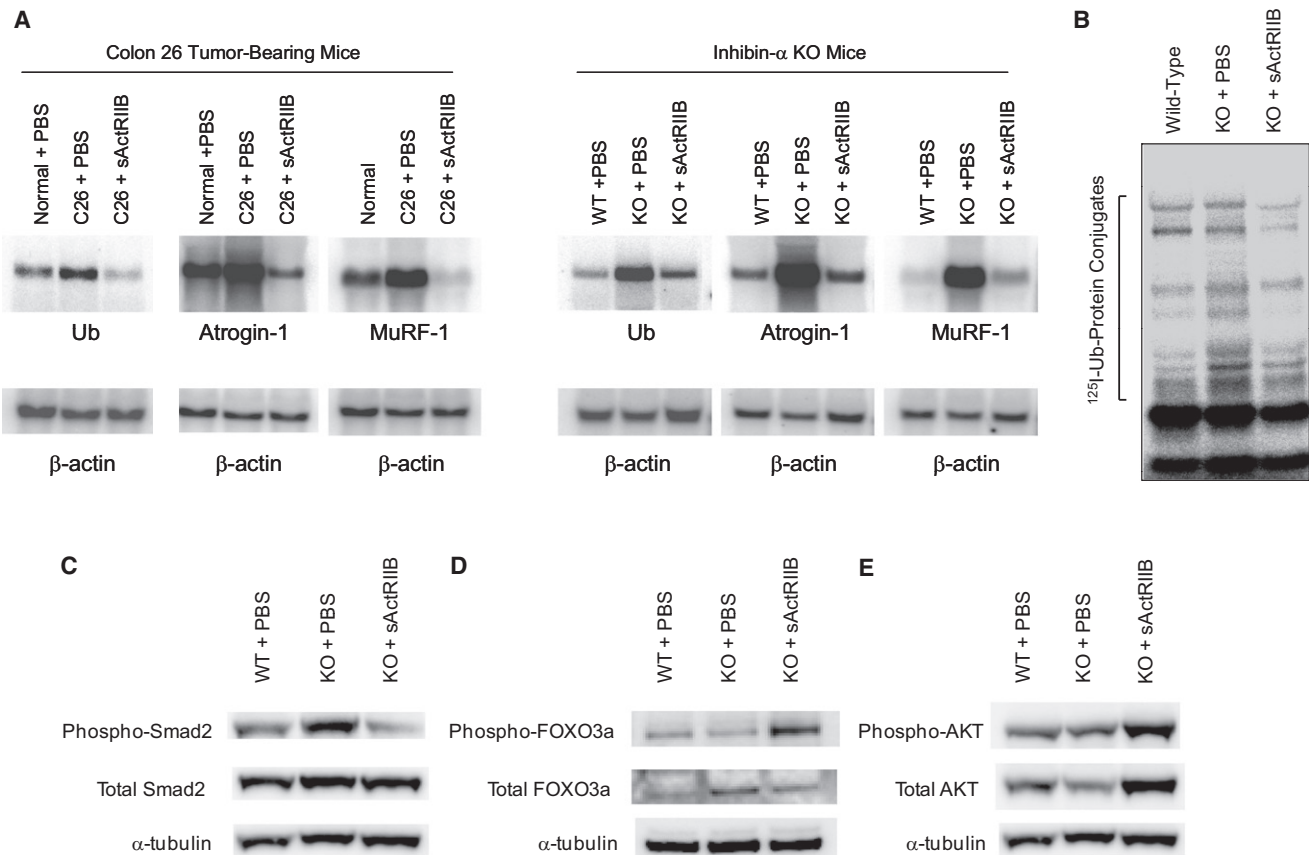
Figure 6. sActRIIB Attenuates the Accelerated Muscle Protein Catabolism during Cancer Cachexia
(A) Northern blot analysis on Ub, Atrogin-1 and MuRF1 in gastrocnemius muscles of C26 mice and inhibin-α KO mice.
(B) sActRIIB inhibits the accelerated Ub-conjugation in atrophying muscle in inhibin-α KO mice.
(C–E) Western blot on Smad2 (C), FOXO3a (D) and AKT (E) in gastrocnemius muscles of inhibin-α KO mice.
n = 8-10.

an increase in AKT activity in the gastrocnemius of the sActRIIB-treated KO mice (Figure 6E). Together, these observations provide strong direct evidence that enhanced Smad2 activity activates FOXO3a signaling in muscle and helps to explain the profound inhibition by sActRIIB of Atrogin-1 and MuRF1 induction.

ActRIIB Pathway Inhibition Stimulates Muscle Stem Cell Growth in Atrophied Muscle
Morphometric analysis of the gastrocnemius showed that the average cross-sectional area of myofibers in the inhibin-α KO mice was 42% smaller than that in WT controls (Figure 7A). Two weeks after a single injection of sActRIIB, the average myofiber area in the KO mice was massively increased (by about 110%) and had become 48% larger than in the controls. Thus, sActRIIB treatment not only prevents atrophy but can also cause hypertrophy. This dramatic growth upon blocking the ActRIIB pathway led us to investigate the effects of sActRIIB administration on muscle stem cell activity. The stem cells present in adult muscles are the satellite cells, which reside between the basement membrane and sarcolemma of myofibers as morphologically distinct, mononucleated cells (Mauro, 1961). Satellite cells

are normally quiescent but can proliferate rapidly in response to exercise, injury and various anabolic stimuli to promote muscle hypertrophy or regeneration (Dhawan & Rando, 2005; Kuang & Rudnicki, 2008). Genetic ablation of myostatin has been reported to cause satellite cell activation (McCroskery et al., 2003). To test whether ActRIIB antagonism may activate satellite cells in normal and atrophied muscles, we performed in vivo BrdU labeling and analyzed the cross-sections of muscles for sActRIIB-induced changes in BrdU staining and in satellite cell markers, Pax7 and M-cadherin (Kuang & Rudnicki, 2008; Moore and Walsh, 1993; Relaix et al., 2006). sActRIIB treatment dramatically increased the numbers of BrdU-, Pax7- and M-cadherin-positive nuclei per myofiber in both WT and KO mice (Figures 7B and 7C; Table S2). A small proportion of Pax7-positive nuclei and the majority of the M-cadherin-positive nuclei were doubly labeled for BrdU (Figure 7C). Similar results were obtained in C26 mice (Figure S5). Thus, the ActRIIB-Smad pathway is critical in maintaining the quiescence of satellite cells in both normal and cachectic muscles. Importantly, these findings suggest that in severely atrophied muscles, some quiescent satellite cells with strong proliferative potential are present and can grow rapidly upon ActRIIB blockade.
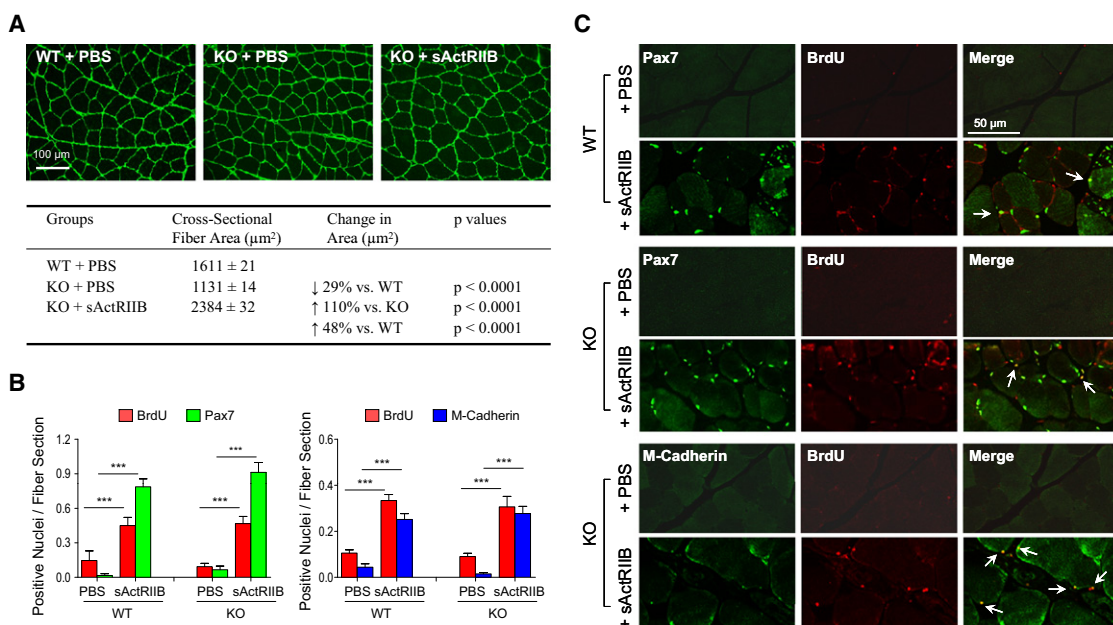
Figure 7. sActRIIB Treatment Increases Myofiber Size and Stimulates Satellite Cell Growth in Normal and Atrophying Muscles

(A) A single dose of sActRIIB rapidly reverses myofiber atrophy in inhibin-α KO mice. WT and KO mice (8-week-old) were treated with sActRIIB (30 mg/kg, SC) or PBS for two weeks. Representative images of the gastrocnemius cross-sections stained with anti-laminin antibody (top) and muscle morphometry data (bottom) are shown.

(B) Counts of BrdU-, Pax7-, and M-cadherin-immunoreactive cells in muscle cross-sections. WT and inhibin-α KO mice received a single injection of PBS or sActRIIB (30 mg/kg, SC) and 7 consecutive daily i.p. injections of BrdU.

(C) Representative images of gastrocnemius cross-sections double-labeled with antibodies against BrdU and Pax7 or BrdU and M-cadherin. Arrows point to double labeled nuclei.

Multiple gastrocnemius sections from 3 individual mice in each group were analyzed by confocal micropscopy. Values are ± SEM. ***p < 0.001.

See also Table S2 and Figure S5.

DISCUSSION

Although cachexia is a highly debilitating syndrome characteristic of many cancers, it remains a poorly understood process whose mechanisms have received only limited attention from cancer researchers. In addition to reducing the patient's quality of life (e.g., strength, endurance, and probably his/her susceptibility to other disease processes), progression of body wasting has poor prognostic implications. In fact, it has often been stated that cachexia is a causative factor in the patients' downhill course, and that a large fraction of cancer deaths is due to this cachectic state. However, direct evidence linking muscle wasting to survival of the tumor-bearing organism has been lacking until now. The present findings in the C26 tumor-bearing mice represent the first clear experimental demonstration that preserving muscle mass is of major importance in determining the organism's survival. In these cachectic mice, ActRIIB antagonism dramatically prolonged survival and not only prevented muscle wasting but even induced net muscle growth, without altering fat mass or growth of the tumor. Therefore, development of treatments that block these catabolic actions of the tumor should be a major therapeutic objective, not just to enhance the quality of life, but also to prolong survival.

The mechanisms signaling the cachectic state have been controversial, and the pathophysiological basis of the muscle wasting in cancer is difficult to unravel. Although the loss of muscle mass clearly can be due to tumor-derived factors, their role is complicated by the associated anorexia, the decreased nutrient supply, and the resulting endocrine changes (e.g., insulin-deficiency, increased glucocorticoids and IGF-1). However, it is now clear that tumor-induced wasting, excessive muscle proteolysis and activation of the ubiquitin proteasome system also occur in pair-fed animals, and a variety of cytokines, especially IL-6, TNF-α and IL-1β, have been proposed to trigger this wasting. However, the present studies fail to support important roles for these factors; in fact, we failed to observe any catabolic effect upon infusion of IL-6. Instead, our findings argue strongly for a dominant role of ActRIIB pathway in the activation of muscle wasting during cancer cachexia: (1) Inhibition of the ActRIIB pathway fully reversed the muscle loss during cancer cachexia, even without affecting the elevated inflammatory cytokine levels; (2) ActRIIB pathway activation induced the ubiquitin ligases critical in muscle wasting and enhanced ubiquitination of muscle proteins, and these effects were completely abolished by sActRIIB; (3) In the tumor-bearing mice, ActRIIB-Smad signaling stimulated FOXO3 activity in muscle, which induced transcription of Atrogin-1 and MuRF1; 4) ActRIIB antagonism dramatically stimulated satellite cell proliferation, which presumably contributes to rapid reversal of muscle loss in the treated animals.

Typically in cachectic organisms, there is a marked loss of both muscle and adipose tissues. It is noteworthy, however, that the dramatic effects of activating or blocking the ActRIIB-Smad pathway on body weight in the C26 tumor-bearing mice involved parallel changes only in the mass of muscles. Moreover, the buildup of muscle correlated with greater myosin expression and increased grip strength. Surprisingly, blocking the ActRIIB pathway in the C26 mice prevented muscle loss or even increased muscle mass above normal levels but did not inhibit adipose tissue loss. Presumably, this continued loss of adipose tissue mass was due to the continued production of other cytokines (e.g., TNF-α) in the C26-bearing animals, since in the inhibin-deficient mice and those bearing activin-secreting CHO tumors, eliminating activin affected muscle and adipose tissue similarly. Thus, the growth and wasting of these two tissues can be regulated in distinct fashions, and only the maintenance of muscle mass correlates with enhanced survival of the cancer-bearing animals.

The present studies have also uncovered a previously unappreciated loss of heart mass in tumor-bearing animals, which is also completely reversed by blocking the ActRIIB pathway. Surprisingly, decreased cardiac size has received virtually no attention in the many recent studies on cancer cachexia, even though early investigators often reported cardiac atrophy in patients with cancer, malnutrition, as well as infections (Hellerstein and Santiago-Stevenson 1950). In C26 tumor-bearing mice and inhibin-deficient mice with gonadal cancers, the heart was found to atrophy by 20%–29%, which approached the loss of skeletal muscle. Furthermore, blocking the ActRIIB pathway completely normalized the heart mass in these tumor-bearing animals. Unlike skeletal muscle, the hearts of the tumor-bearing animals did not show the marked induction of Atrogin-1 or MuRF1. The cellular mechanisms of this severe cardiac atrophy and re-growth and how increased signaling by the ActRIIB pathway influences cardiac size and performance will be important issues for future study. It is noteworthy that myostatin and activin have been implicated in cardiac failure (Heineke et al., 2010; Rodgers et al., 2009; Springer et al., 2010; Yndestad et al., 2004). Presumably, the reversal of cardiac atrophy, in addition to the restoration of skeletal muscle, contributed to the prolongation of lifespan in the tumor-bearing animals seen upon ActRIIB blockade. Further studies will be needed to evaluate the functional impact of cancer-induced heart atrophy, as well as its reversal by sActRIIB, to cardiac performance.

As noted above, cancer cachexia is also associated with anorexia, which may also contribute to the loss of muscle mass and the patient's downhill course. In the present studies, the ActRIIB treatment markedly stimulated food intake in the inhibin-deficient mice, the activin-secreting CHO tumors, and human tumor xenografts-bearing mice back to or above control levels. These findings indicate that enhanced activin signaling reduces appetite and food intake, but the mechanisms for this marked effect remain to be elucidated. Although increased nutrient intake probably played some role in the dramatic muscle growth and enhancing survival, our studies on pair-fed animals indicate that the decreased food intake in response to high circulating levels of activin A accounts at most for a small fraction of the loss of body weight (Figure S4A), and thus enhanced tissue catabolism seems a more important cause of the wasting syndrome.

While these insights advance our understanding of the importance of ActRIIB pathway in the pathogenesis of the cachexia-anorexia syndrome, additional investigations will obviously be required to clarify the therapeutic value of ActRIIB antagonism in treating the debilitating wasting associated with diverse tumor types and non-malignant diseases (e.g., AIDS, sepsis, burns, cardiac and renal failure). Numerous reports have documented increased expression of activin A in cancer patients (Harada et al., 1996; Otani et al., 2001; Petraglia et al., 1998; Seder et al., 2009; Thomas, et al., 1997; Wildi et al., 2001), for example, in patients with solid cancers (Harada et al., 1996) and ones with endometrial and cervical carcinoma (Petraglia et al., 1998). In the present studies, about a third of the human tumor xenografts examined were found to produce large amounts of activin A (Figure 5B). Elevated serum activin A has also been reported in patients in various non-malignant diseases, including patients with renal failure, heart failure and hyperthyroidism (Harada et al., 1996; Yndestad et al., 2004).

While these findings point to a systemic activation of this highly catabolic factor in patients with wasting syndromes, further clinical studies will be needed to define the precise role of activin A in the cachexia-anorexia syndrome with cancer and non-malignant diseases and possible contributions of other factors. Little is known presently about myostatin's levels in various human diseases, in part due to the lack of a sensitive assay of human myostatin. It will also be important to determine the levels of other ActRIIB pathway ligands and regulatory factors (e.g., inhibin-α, propeptide and follistatin) in different cohorts of patients. The dramatic, reversible changes in body mass shown here emphasize the importance of obtaining such information not only for understanding disease mechanisms but also to provide a fuller rationale basis for anti-activin therapies. However, since the inhibition of ActRIIB signaling by sActRIIB induces growth of normal muscle (Figure S1B), this treatment is likely to be anabolic and help combat muscle loss in many catabolic conditions, even if the wasting is not triggered by excessive signaling by activin or related ligands of the ActRIIB pathway.

EXPERIMENTAL PROCEDURES

Materials

sActRIIB

The sActRIIB (soluble ActRIIB-Fc) expression construct was engineered by subcloning a cDNA fragment corresponding to the extracellular domain of human activin type-2B receptor (aa 7–100) into an IgG2 Fc fusion split vector. The construct was transfected into CHO cells and the recombinant sActRIIB was purified from culture medium using a mAb Select SuRe affinity column (GE) followed by Fractogel chromatography (EMD Chemicals).

Anti-Activin A Antibody

Monoclonal anti-activin A antibody was generated in XenoMouse (Amgen Inc) using recombinant activin A as an immunogen.

Recombinant IL-6

hu-IL-6 was expressed and purified using mammalian expression system (Amgen Inc).

Smad 2/3 Reporter Assay

Smad2/3 luciferase reporter construct pLuc-MCS(CAGA)$_{12}$ was engineered by subcloning a repeat of twelve GAGA elements into pLuc-MCS (Strategen).

Stably transfected C2C12 myoblasts were used to measure the neutralizing activity of sActRIIB against myostatin or activin A by luciferase assay (Promega).

Cell Cultures

The TOV-21G and G361 human cancer cell lines (ATCC) were cultured in RPMI 1640 medium supplemented with 10% FBS. CHO cells were cultured in DMEM supplemented with 10% FBS (Invitrogen).

Animal Models

Ethics Committee Approval

All mouse experiments were performed with the approval of Institutional Animal Care and Use Committee and are in accordance with the NIH Guide for the Care and Use of Laboratory Animals.

C26 Tumor-Bearing Mice

The colon 26 murine adenocarcinoma cells were subcutaneously inoculated into the flank region of 10-week-old male CDF1 mice (0.5×10^6 cells/mouse). C26 implanted mice were treated with sActRIIB or PBS at different time points. Multiple experiments were performed with body weight, body composition, tumor size, grip strength, and survival rates recorded. Weights of lean carcass, muscle and tumor were measured via necropsy.

IL-6 infusion

CDF1 mice were infused with recombinant IL-6 or saline (n = 12) by using osmotic pump (Alzet) at a rate of 1 μl/hr (7.2 μg/day) and analyzed at day 1, 3, and 5 for serum IL-6 exposure levels and changes in body weight and muscle mass.

Inhibin-α KO Mice

For survival studies, 8-week-old KO mice received sActRIIB (10 mg/kg, weekly, SC) or PBS with body weights and survival rates recorded. For single-dose studies, 8-weak-old male and 12-week-old female KO mice were treated with sActRIIB (30 mg/kg, SC) or PBS for 2 weeks. Changes in body weight, food intake, body composition and grip strength, and terminal muscle mass were measured.

Activin A Xenograft-Bearing Mice

CHO cells were stably transfected with activin A expression construct (CHO-Activin) or vector (CHO-Vector). 3×10^6 cells were implanted intramuscularly (right quadriceps) in each CD1 nude mouse (CRL). CHO-Activin xenograft mice were treated with PBS or anti-activin A antibody immediately after implantation.

TOV-21G and G361 Xenografts-Bearing Nude Mice

5×10^6 cells of each tumor lines were inoculated subcutaneously into each athymic or BALB/c nu/nu mouse (Harlan, and CRL). Treatment began at day 12 or 18 after implantation, when the average sizes of TOV-21G and G361 reached 150 mm^3 and 130 mm^3, respectively.

Body Composition, Muscle Grip Strength, and Tumor Size

Lean body mass and fat mass were measured using nuclear magnetic resonance (NMR; Echo Medical Systems). Forelimb grip strength was measured with Digital Grip strength meter (Columbus Instruments). Five measurements with 3 min interval between tests were completed for each mouse. Tumor size was measured by electronic caliper. Tumor volume (mm^3) was based on tumor length (mm) x width (mm) x height (mm). Terminal tumor weights were determined by necropsy.

Western Blot

Equal amounts of total protein extracts (30 μg $-$100 μg) derived from the gastrocnemius muscles of individual mouse groups were separated by NuPAGE (Invitrogen), transferred to PVDF membrane and probed with antibodies against Smad 2, phospho-Smad 2, FOXO3a, phospho-FOXO3a, and AKT (1:1000; Cell Signaling) or myosin heavy chain and phospho-AKT (1:200; Abcam). The membranes were stripped and re-probed with antibody against α-tubulin (1:2000; Cell Signaling).

Northern Blot

A pool of 10 μg RNA derived from the gastrocnemius muscles of each mouse group was fractionated by the Northern gel and probed (see Extended Experimental Procedures and Table S3).

Ub-Conjugation Assay

Extracts of gastrocnemius muscles were prepared for each mouse group. Soluble fractions of the extract proteins were subjected to Ub-conjugation assays by incubating 30 μg of extracts with ^{125}I-Ub (0.15 mg/ml; $\sim$1 $\times$ 10^7 cpm) at 37°C for 1 hr in buffer containing 20 mM Tris, (pH 7.5)/1 mM DTT/5 mM $MgCl_2$/2 mM adenosine 5'-[γ-thio]triphosphate (ATPγS), 0.1 mM MG-132/0.02 mM ubiquitin aldehyde. The reaction mixtures were fractionated by SDS-PAGE and autoradiographed (See Extended Experimental Procedures).

ELISA

Serum myostatin and activin A were assayed by sandwich ELISA employing a non-competing pair of antibodies for each ligand as described in Extended Experimental Procedures. Serum TNF-α, IL-1β and IL-6 levels were measured by using Milliplex MAP mouse cytokine assay kit (Millipore).

Histology

Frozen muscle sections of 8 μm in thickness and formalin-fixed cardiac sections of 4 μm in thickness were prepared and used (see Extended Experimental Procedures).

Immunofluorescence Staining of Satellite Cells

Muscle sections in vivo-labeled with BrdU were subjected to immunofluorescence labeling with antibodies against BrdU, Pax7 and M-cadherin and analyzed as detailed in Extended Experimental Procedures.

Statistics

Groups of tissue weights were compared using Student's t test. Longitudinal body weight or muscle mass differences were analyzed by repeated-measurement ANOVA. Survival rate difference was determined by Chi-Square test. P values < 0.05 were considered significant.

SUPPLEMENTAL INFORMATION

Supplemental information includes Extended Experimental Procedures, five figures, and three tables can be found with this article online at doi:10.1016/j.cell.2010.07.011.

REFERENCES

Acharyya, S., Butchbach, M., Sahenk, Z., Wang, H., Saji, M., Carathers, M., Ringel, M., Skipworth, R., Fearon, K., and Hollingsworth, M. (2005). Dystrophin glycoprotein complex dysfunction: A regulatory link between muscular dystrophy and cancer cachexia. Cancer Cell 8, 421–432.

Argiles, J.M., and Lopez-Soriano, F.J. (1999). The role of cytokines in cancer cachexia. Med. Res. Rev. 19, 223–248.

Bodine, S.C., Latres, E., Baumhueter, S., Lai, V.K., Nunez, L., Clarke, B.A., Poueymirou, W.T., Panaro, F.J., Na, E., Dharmarajan, K., et al. (2001).

Identification of ubiquitin ligases required for skeletal muscle atrophy. Science *294*, 1704–1708.

Cipriano, S.C., Chen, L., Kumar, T.R., and Matzuk, M.M. (2000). Follistatin is a modulator of gonadal tumor progression and the activin-induced wasting syndrome in inhibin-deficient mice. Endocrinology *141*, 2319–2327.

Coerver, K.A., Woodruff, T.K., Finegold, M.J., Mather, J., Bradley, A., and Matzuk, M.M. (1996). Activin signaling through activin receptor type II causes the cachexia-like symptoms in inhibin-deficient mice. Mol. Endocrinol. *10*, 534–543.

Cohen, S., Brault, J.J., Gygi, S.P., Glass, D., Valenzuela, D.M., Gartner, C., Latres, E., and Goldberg, A.L. (2009). During muscle atrophy, thick, but not thin filament components are degraded by MuRF1-dependent ubiquitylation. J. Cell Biol. *185*, 1083–1095.

Costelli, P., Muscaritoli, M., Bonetto, A., Penna, F., Reffo, P., Bossola, M., Bonelli, G., Doglietto, G.B., Baccino, F.M., and Fanelli, F.R. (2008). Muscle myostatin signalling is enhanced in experimental cancer cachexia. Eur. J. Clin. Invest. *38*, 531–538.

Dhawan, J., and Rando, T.A. (2005). Stem cells in postnatal myogenesis: molecular mechanisms of satellite cell quiescence, activation and replenishment. Trends Cell Biol. *15*, 666–673.

Fearon, K.C. (2008). Cancer cachexia: developing multimodal therapy for a multidimensional problem. Eur. J. Cancer *44*, 1124–1132.

Glass, D.J. (2005). Skeletal muscle hypertrophy and atrophy signaling pathways. Int. J. Biochem. Cell Biol. *37*, 1974–1984.

Gomes, M.D., Lecker, S.H., Jagoe, R.T., Navon, A., and Goldberg, A.L. (2001). Atrogin-1, a muscle-specific F-box protein highly expressed during muscle atrophy. Proc. Natl. Acad. Sci. USA *98*, 14440–14445.

Harada, K., Shintani, Y., Sakamoto, Y., Wakatsuki, M., Shitsukawa, K., and Saito, S. (1996). Serum immunoreactive activin A levels in normal subjects and patients with various diseases. J. Clin. Endocrinol. Metab. *81*, 2125–2130.

Heineke, J., Auger-Messier, M., Xu, J., Sargent, M., York, A., Welle, S., and Molkentin, J.D. (2010). Genetic Deletion of Myostatin From the Heart Prevents Skeletal Muscle Atrophy in Heart Failure. Circulation *121*, 419–425.

Hellerstein, H.K., and Santiago-Stevenson, D. (1950). Atrophy of the Heart: A Correlative Study of Eighty-Five Proved Cases. Circulation *1*, 93–126.

Kuang, S., and Rudnicki, M.A. (2008). The emerging biology of satellite cells and their therapeutic potential. Trends Mol. Med. *14*, 82–91.

Kwak, K.S., Zhou, X., Solomon, V., Baracos, V.E., Davis, J., Bannon, A.W., Boyle, W.J., Lacey, D.L., and Han, H.Q. (2004). Regulation of protein catabolism by muscle-specific and cytokine-inducible ubiquitin ligase E3alpha-II during cancer cachexia. Cancer Res. *64*, 8193–8198.

Lee, S.J., and McPherron, A.C. (2001). Regulation of myostatin activity and muscle growth. Proc. Natl. Acad. Sci. USA *98*, 9306–9311.

Lee, S.J., Reed, L.A., Davies, M.V., Girgenrath, S., Goad, M.E., Tomkinson, K.N., Wright, J.F., Barker, C., Ehrmantraut, G., Holmstrom, J., et al. (2005). Regulation of muscle growth by multiple ligands signaling through activin type II receptors. Proc. Natl. Acad. Sci. USA *102*, 18117–18122.

Li, Q., Kumar, R., Underwood, K., O'Connor, A.E., Loveland, K.L., Seehra, J.S., and Matzuk, M.M. (2007). Prevention of cachexia-like syndrome development and reduction of tumor progression in inhibin-deficient mice following administration of a chimeric activin receptor type II-murine Fc protein. Mol. Hum. Reprod. *13*, 675–683.

Mammucari, C., Milan, G., Romanello, V., Masiero, E., Rudolf, R., Del Piccolo, P., Burden, S.J., Di Lisi, R., Sandri, C., Zhao, J., et al. (2007). FoxO3 controls autophagy in skeletal muscle in vivo. Cell Metab. *6*, 458–471.

Matzuk, M.M., Finegold, M.J., Mather, J.P., Krummen, L., Lu, H., and Bradley, A. (1994). Development of cancer cachexia-like syndrome and adrenal tumors in inhibin-deficient mice. Proc. Natl. Acad. Sci. USA *91*, 8817–8821.

Mauro, A. (1961). Satellite cell of skeletal muscle fibers. J. Biophys. Biochem. Cytol. *9*, 493–495.

McCroskery, S., Thomas, M., Maxwell, L., Sharma, M., and Kambadur, R. (2003). Myostatin negatively regulates satellite cell activation and self-renewal. J. Cell Biol. *162*, 1135–1147.

Mitch, W.E., and Goldberg, A.L. (1996). Mechanisms of muscle wasting. The role of the ubiquitin-proteasome pathway. N. Engl. J. Med. *335*, 1897–1905.

Moore, R., and Walsh, F.S. (1993). The cell adhesion molecule M-cadherin is specifically expressed in developing and regenerating, but not denervated skeletal muscle. Development *117*, 1409–1420.

Mori, M., Yamaguchi, K., Honda, S., Nagasaki, K., Ueda, M., Abe, O., and Abe, K. (1991). Cancer cachexia syndrome developed in nude mice bearing melanoma cells producing leukemia-inhibitory factor. Cancer Res. *51*, 6656–6659.

Otani, T., Minami, S., Yamoto, M., and Umesaki, N. (2001). Production of activin A in hyperplasia and adenocarcinoma of the human endometrium. Gynecol. Oncol. *83*, 31–38.

Petraglia, F., Florio, P., Luisi, S., Gallo, R., Gadducci, A., Viganò, P., Di Blasio, A.M., Genazzani, A.R., and Vale, W. (1998). Expression and secretion of inhibin and activin in normal and neoplastic uterine tissues. High levels of serum activin A in women with endometrial and cervical carcinoma. J. Clin. Endocrinol. Metab. *83*, 1194–1200.

Provencher, D.M., Lounis, H., Champoux, L., Tetrault, M., Manderson, E.N., Wang, J.C., Eydoux, P., Savoie, R., Tonin, P.N., and Mes-Masson, A.M. (2000). Characterization of four novel epithelial ovarian cancer cell lines. In Vitro Cell. Dev. Biol. *36*, 357–361.

Relaix, F., Montarras, D., Zaffran, S., Gayraud-Morel, B., Rocancourt, D., Tajbakhsh, S., Mansouri, A., Cumano, A., and Buckingham, M. (2006). Pax3 and Pax7 have distinct and overlapping functions in adult muscle progenitor cells. J. Cell Biol. *172*, 91–102.

Rodgers, B.D., Interlichia, J.P., Garikipati, D.K., Mamidi, R., Chandra, M., Nelson, O.L., Murry, C.E., and Santana, L.F. (2009). Myostatin represses physiological hypertrophy of the heart and excitation-contraction coupling. J. Physiol. *15*, 4873–4886.

Sandri, M., Sandri, C., Gilbert, A., Skurk, C., Calabria, E., Picard, A., Walsh, K., Schiaffino, S., Lecker, S.H., and Goldberg, A.L. (2004). Foxo transcription factors induce the atrophy-related ubiquitin ligase atrogin-1 and cause skeletal muscle atrophy. Cell *117*, 399–412.

Sartori, R., Milan, G., Patron, M., Mammucari, C., Blaauw, B., Abraham, R., and Sandri, M. (2009). Smad2 and 3 transcription factors control muscle mass in adulthood. Am. J. Physiol. Cell Physiol. *296*, C1248–C1257.

Schuelke, M., Wagner, K.R., Stolz, L.E., Hubner, C., Riebel, T., Komen, W., Braun, T., Tobin, J.F., and Lee, S.J. (2004). Myostatin mutation associated with gross muscle hypertrophy in a child. N. Engl. J. Med. *350*, 2682–2688.

Seder, C.W., Hartojo, W., Lin, L., Silvers, A.L., Wang, Z., Thomas, D.G., Giordano, T.J., Chen, G., Chang, A.C., Orringer, M.B., et al. (2009). Upregulated INHBA expression may promote cell proliferation and is associated with poor survival in lung adenocarcinoma. Neoplasia *11*, 388–396.

Seoane, J., Le, H.V., Shen, L., Anderson, S.A., and Massague, J. (2004). Integration of Smad and forkhead pathways in the control of neuroepithelial and glioblastoma cell proliferation. Cell *117*, 211–223.

Solomon, V., Baracos, V., Sarraf, P., and Goldberg, A.L. (1998). Rates of ubiquitin conjugation increase when muscles atrophy, largely through activation of the N-end rule pathway. Proc. Natl. Acad. Sci. USA *95*, 12602–12607.

Souza, T.A., Chen, X., Guo, Y., Sava, P., Zhang, J., Hill, J.J., Yaworsky, P.J., and Qiu, Y. (2008). Proteomic identification and functional validation of activins and bone morphogenetic protein 11 as candidate novel muscle mass regulators. Mol. Endocrinol. *22*, 2689–2702.

Springer, J., Adams, V., and Anker, S.D. (2010). Myostatin: Regulator of Muscle Wasting in Heart Failure and Treatment Target for Cardiac Cachexia. Circulation *121*, 354–356.

Strassmann, G., Fong, M., Kenney, J.S., and Jacob, C.O. (1992). Evidence for the involvement of interleukin 6 in experimental cancer cachexia. J. Clin. Invest. *89*, 1681–1684.

Tanaka, Y., Eda, H., Tanaka, T., Udagawa, T., Ishikawa, T., Horii, I., Ishitsuka, H., Kataoka, T., and Taguchi, T. (1990). Experimental cancer cachexia induced by transplantable colon 26 adenocarcinoma in mice. Cancer Res. *50*, 2290–2295.

Tanaka, M., Miyazaki, H., Takeda, Y., and Takeo, S. (1993). Detection of serum cytokine levels in experimental cancer cachexia of colon 26 adenocarcinoma-bearing mice. Cancer Lett. *72*, 65–70.

Thomas, T.Z., Wang, H., Niclasen, P., Obryan, M.K., Evans, L.W., Groome, N.P., Pedersen, J., and Risbridger, G.P. (1997). Expression and localization of activin subunits and follistatins in tissues from men with high grade prostate cancer. J. Clin. Endocrinol. Metab. *82*, 3851–3858.

Tisdale, M.J. (2009). Mechanisms of cancer cachexia. Physiol. Rev. *89*, 381–410.

Trendelenburg, A.U., Meyer, A., Rohner, D., Boyle, J., Hatakeyama, S., and Glass, D.J. (2009). Myostatin reduces Akt/TORC1/p70S6K signaling, inhibiting myoblast differentiation and myotube size. Am. J. Physiol. Cell Physiol. *296*, C1258–C1270.

Wildi, S., Kleeff, J., Maruyama, H., Maurer, C.A., Buchler, M.W., and Korc, M. (2001). Overexpression of activin A in stage IV colorectal cancer. Gut *49*, 409–417.

Yndestad, A., Ueland, T., Øie, E., Florholmen, G., Halvorsen, B., Attramadal, H., Simonsen, S., Frøland, S.S., Gullestad, L., Christensen, G., et al. (2004). Elevated Levels of Activin A in Heart Failure: Potential Role in Myocardial Remodeling. Circulation *109*, 1379–1385.

Zhao, J., Brault, J.J., Schild, A., Cao, P., Sandri, M., Schiaffino, S., Lecker, S.H., and Goldberg, A.L. (2007). FoxO3 coordinately activates protein degradation by the autophagic/lysosomal and proteasomal pathways in atrophying muscle cells. Cell Metab. *6*, 472–483.

Zimmers, T.A., Davies, M.V., Koniaris, L.G., Haynes, P., Esquela, A.F., Tomkinson, K.N., McPherron, A.C., Wolfman, N.M., and Lee, S.J. (2002). Induction of cachexia in mice by systemically administered myostatin. Science *296*, 1486–1488.